Analysis of Friction Stir Welds. Part I: Transient Thermal Simulation Using Moving Heat Source

Prof. Dr. Qasim M. Doos
Mechanical Engineering Dep. / Baghdad University

Prof. Dr. Muhsin Jabir Jweeg
Mechanical Engineering Dep. / Nahrain University

Sarmad Dhia Ridha
Mechanical Engineering Dep. / Baghdad University

Abstract:

This paper describes the first part of the development of a non-linear finite element simulation of the friction stir welding process; it is concerned with thermal analysis. A transient, three dimensional, non-linear thermal model with moving heat source was developed. Also a steady-state, three dimensional, non-linear fluid-thermal model with stationary heat source was developed. Differences of results for both models were discussed. Results of both models were compared with experimental work. Transient thermal model results appear to be more reliable as compared to the CFD approach.

Introduction

Friction stir welding (FSW) is a solid-state joining technique invented by TWI that is effective for metallic and nonmetallic materials [1]. The process advantages result principally from the fact that temperatures remain below the melting point of the materials being joined. The benefits include the ability to join materials which are difficult to fusion weld, for example 2000 and 7000 aluminum alloys. Other advantages are low shrinkage and distortion, excellent mechanical properties, and low production of fumes.

A FSW process commences by inserting a spinning tool pin into the surface of adjoining parts. The tool pin shoulder presses against the workpieces and helps contain the material flow.

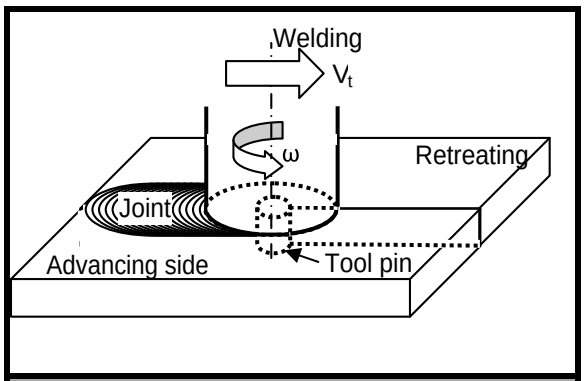

Figure 1. A schematic diagram of the FSW system

The tool rotates rapidly, inducing complicated material flow patterns and highly altering the microstructures (Figure 1)

The heat transfer process is one of the most important aspects in the FSW study. This is because .A good understanding of the heat transfer process in the workpiece can be helpful in predicting

Nomenclature

T_o	Initial plate temperature [K]
v	Viscosity [N/m.sec]
$\dot{Q}$	Heat generation term [W/m^3]
$\vec{u}$	Velocity vector
p	Pressure
k	Thermal conductivity
c_p	Specific heat
u_x	Velocity in x-direction
u_y	Velocity in y-direction
T	Temperature [K]
T_a	Ambient temperature [K]
X	Tool location [mm]
i	Time index
V_t	Tool traveling speed [mm/sec]
h_b	Convection heat transfer coefficient with backing plate [W/m^2.K]
h	Convection heat transfer coefficient with surrounding [W/m^2.K]

ε	Emissivty
σ	STEFAN BOLTZMANN constant [W/m^2.K]
ω	Tool rotational speed [rad/sec]
ρ	Density [kg/m$^{3]}$
δ	Slip factor
Δ	The Laplacian
∇	Divergence operator

the thermal cycles in the welding work piece, and the hardness in the weld zone, subsequently, can be helpful in evaluating the weld quality.

Several papers have been written on the FSW thermal process, some of them were seeking for analytical solution [2] while the other uses numerical methods to solve the problem. In this work, numerical method was used. To our knowledge, none has attempt a comparative study on solid-thermal analysis verses fluid thermal one. Also limitations of both approaches has not been discussed any where else.

Ulysse [3] presents an attempt to numerically model the stir-welding process using three-dimensional visco-plastic modeling. The scope of his project is focused on butt joints for aluminum thick plates. He conducted a parametric study to determine the effect of tool speeds on plate temperatures and to validate the model predictions with available measurements..

M. Song and R. Kovacevic [4] presented a three-dimensional heat transfer model for friction stir welding (FSW). A moving coordinate is introduced in this work to reduce the difficulty of modeling the moving tool. Heat input from the tool shoulder and the tool pin are considered in the model. The finite difference method was applied in solving the control equations. A non-uniform grid mesh is generated for the calculation.

Vijay Soundararajan et al. [5] focuses there work on contact conductance, which depends on the pressure at the interface and it has a non-uniform variation. The actual pressure distribution along the interface is dependent on the thermal stress from local temperature and non-linear stress–strain state.

In R. Nandan et al. [6], a three-dimensional visco-plastic flow of metals and the temperature fields in friction stir welding have been modeled based on the previous work on thermomechanical processing of metals. The equations of conservation of mass, momentum, and energy were solved in three dimensions using spatially variable thermophysical properties and non-Newtonian viscosity.

In this work, two mathematical models were solved using ANSYS. First, a steady state fluid-thermal model was solved to study the flow of material and temperature distributions a result of tool movement. The second model was a transient thermal model with moving heat source, this model is necessary for the subsequently structural analysis. The reason behind the use of two models or approaches is to define the inherent characteristics of each approach.

By reason of assessment and to reduces the number of finite element approach variables, the plate was modeled in both analysis approach with the same dimensions, which are given in table 1, and the same cube element with edge length (element size) of 0.5 mm. With 0.5mm element size, numerical stability and results convergence test was found to be satisfied and adequate for both models.

2- Mathematical Modeling

2.1 Governing Equations

The continuity equation for incompressible single-phase flow is given by [7]:

$$\nabla \cdot \vec{u} = 0 \qquad (1)$$

and conservation of momentum [7]:

$$\frac{\partial \vec{u}}{\partial t} + (\vec{u} \cdot \nabla)\vec{u} = -\frac{1}{\rho}\nabla p + \nu \Delta \vec{u} \qquad (2)$$

The temperature generated in FSW process can be quite high and have a considerable influence on the mechanical response. This heat generation and transfer is expressed in the form of energy balance as follows [7],

$$\rho c_p \frac{dT}{dt} = \nabla (k \nabla T) + \dot{Q} \qquad (3)$$

As mentioned earlier, in this paper two models were built. In building the fluid-thermal model, all the above three equations were used to simulate the FSW process. While in the second model, thermal model with moving heat source, only the energy equation (3) was used. The boundary conditions

associated with each model will be mentioned next.

2.2 Boundary condition and Thermo-physical properties

2.2.1 Thermal Boundary Conditions

Figure 2 shows the main thermal boundary conditions used in both models.

The boundary condition for the heat exchange between the workpiece and the surroundings beyond the shoulder involved consideration of both convection and radiation heat transfer

$$k\frac{\partial T}{\partial x_i} = h\left(T - T_a\right) + \sigma\varepsilon\left(T^4 - T^4{}_a\right) \quad (4)$$

Where, x_1= z for top surface, and x_1= x or y for side surfaces. σ is the Stefan-Boltzmann constant, ε is the emissivity, h is the convection heat transfer coefficient, and Ta is the ambient temperature. At the bottom surface, the heat transfer coefficient based on the previously reported value [6] was used

$$k\frac{\partial T}{\partial z} = h_b\left(T - T_a\right) \quad (5)$$

Both of these boundary conditions were used in both models

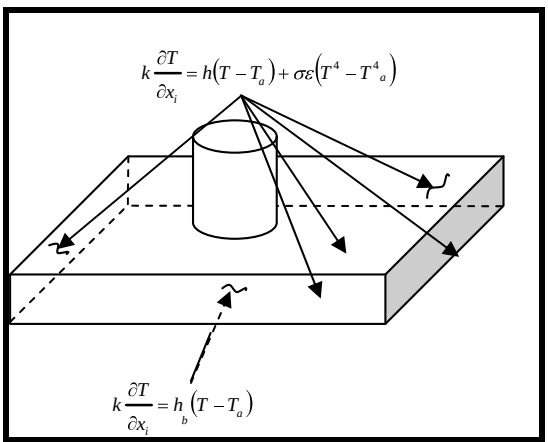

Figure 2. Thermal boundary condition

The workpiece in FSW process is heated by two sources. First source is the frictional heat that released because of friction between faces that interfaces the workpiece. This part of the heating load was proved in experiments to be more than 90% of the total heat generated in the process [3]. The second source is the heat that released due to plastic flow in the stirring zone. In this work only the first source will be used. It form of variation was taking according the work reported by R. NANDAN [6]. The variation of this type of heating load is shown in figure 3.

2.2.2 Thermo-physical properties

In an ideal case, Thermo-physical properties values over the entire gamut of temperature from room condition all the way up to the melting point are required for an accurate simulation. Thermo-physical properties includes: specific heat, thermal conductivity, and density. Figure 4 shows variation of specific heat and thermal conductivity with temperature for Al6061 as was taken from J.E. Gould [6]. Density and viscosity were constant.

According to Paul A et al. viscosity variation are strongly related to the strain rate, which in turn has high gradient under shoulder zone. This work is focused on the overall temperature distribution and frictional heating load was taken the main source. Hence, a constant value of viscosity could be used. R. NANDAN et al. shows that variation of viscosity was between 10^6 to $4e10^6$. This variation of viscosity was reported to be underneath the shoulder zone. No flow was apparent for viscosity values above $4e10^6$. Viscosity was fixed to $3e10^6$ through this work.

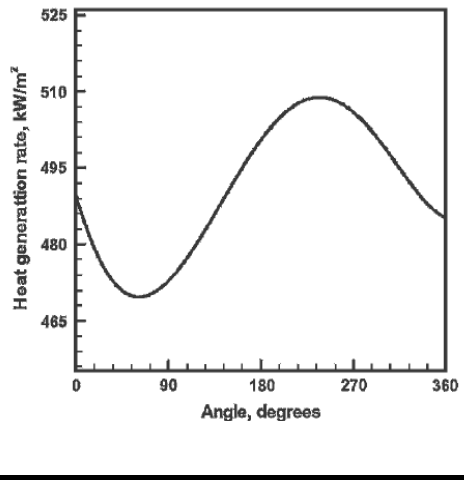

Figure 3. Variation of frictional heating load [6].

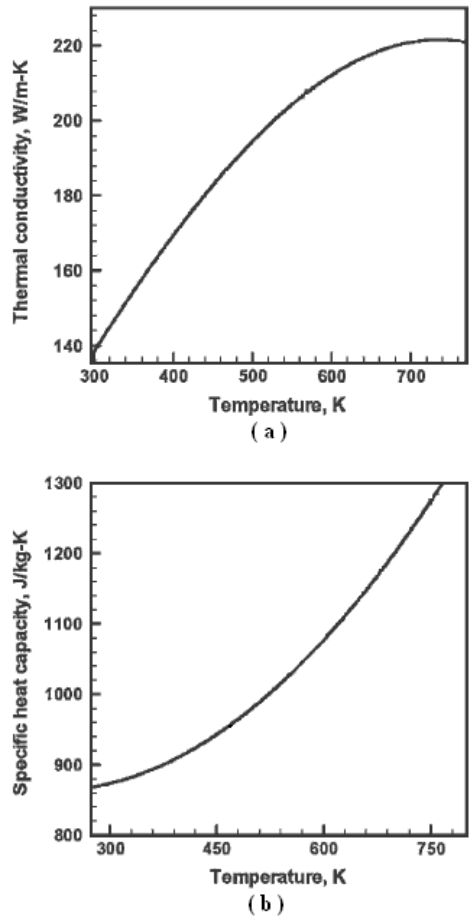

Figure 4. Variation of Thermo-physical properties with temperature [6].

2.2.3 Fluid Boundary Conditions

Continuity and momentum equations were solved numerically by using ANSYS package. The boundary conditions used in this work are shown in Figure 5. Instead of simulating the tool movement during the process, the workpiece was assumed to move. This assumption was performed by simulating be a duct that contains a moving fluid having Thermo-physical properties of the workpiece metal. At side walls no slip condition was used (i.e. $u_x=u_y= 0$). Velocity at the entrance was taken to be equal to the tool translation velocity with normal velocities equal to zero (i.e. $u_x=V_t$, $u_y=0$). At the duct exit the only fluid boundary condition was $u_x=V_t$. Velocity on upper and lower faces was not included in the selected boundary conditions.

Under the shoulder the velocity boundary condition was taken to follow the form (with reference to Fig. 6)

$u_x = -(1-\delta)\ \omega\ r \sin(\theta) - V_t$ $u_y = (1-\delta)\ \omega\ r \cos(\theta)$	6

where δ is the slip factor . Figure 6 shows the velocity profile given by the above equations.

3. Results and Discussion

3.1 Fluid-Thermal Model

In this work ANSYS package was used in modeling the FSW process. The element was FLUID142. FLUID142 could be used to model transient or steady state fluid/thermal systems [8] that involve fluid and/or non-fluid regions. The conservation equations for viscous fluid flow and energy are solved in the fluid region. For the FLOTRAN CFD elements (e.g. FLUID142) the velocities are obtained from the conservation of momentum principle,

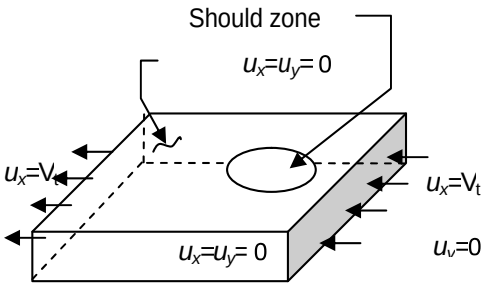

Figure 5. Fluid boundary condition

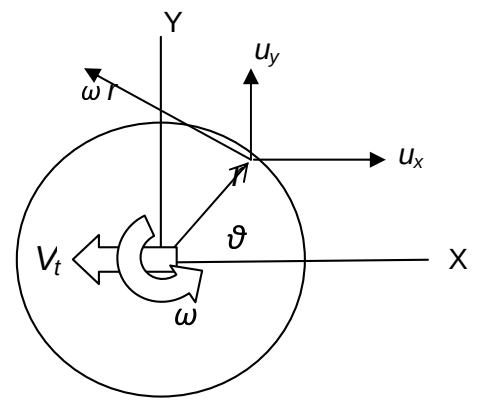

Figure 6. Top view of the tool showing velocity boundary conditions at the tool surface.

and the pressure is obtained from the conservation of mass principle. The temperature distribution is obtained from the

law of conservation of energy. Rate of change of temperature was discarded. Boundary conditions, which were described in section (2.2.3), were implemented. Thermo-physical properties, which were described in section (2.2.2), were used. Heat source location was fixed at quarter the length of the workpiece near fluid entrance side.

Figure 7 shows the stream line representation of the flow. The effect of tool rotation on the flow is apparent. Walls shear effect is the main reason behind the concave form of the stream lines.

ure 8 shows the temperatures field while material absolute velocities are shown in figure 9. It is clearly observed that the heat is concentrated at the shoulder surface, where the largest deformation rates are produced, and as a consequence to the greatest heat generation.

Figure 10 and figure 11 show the velocity distribution in x-direction and y-direction respectively. The straight lines that enclosed between maximum and minimum values represent the velocity underneath the shoulder face. While curved lines of the plot represents the effect of tool rotation on the tool closest flow (workpiece). The horizontal line for u_y = 0 in figure 11 shows how

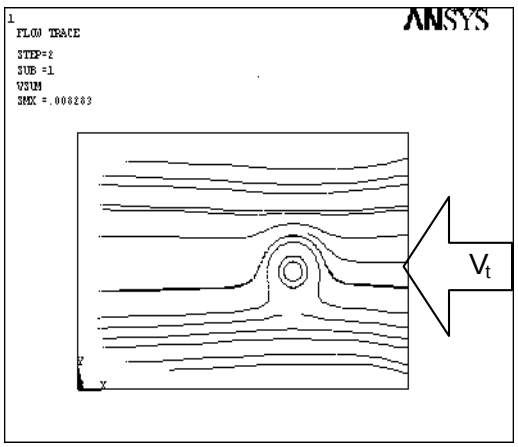

Figure 7. Flow representation by stream lines

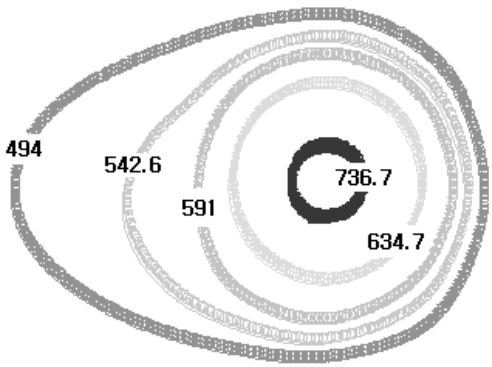

Figure 8. Temperature field for fluid- thermal model

This figure shows also that the effect of heating load shown in figure 3 has no noticeable affect on the temperature distribution. The temperature distribution is therefore appearing to be symmetric about the workpiece center line. Other data used in fluid-thermal

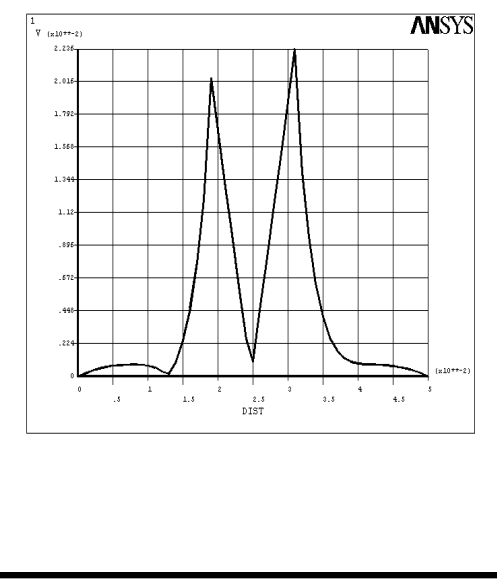

Figure 9. Material absolute velocities Section 2

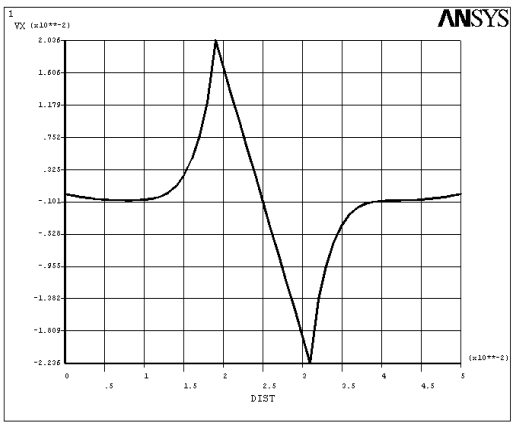

Figure 10. Velocity component in x-direction. Section 3

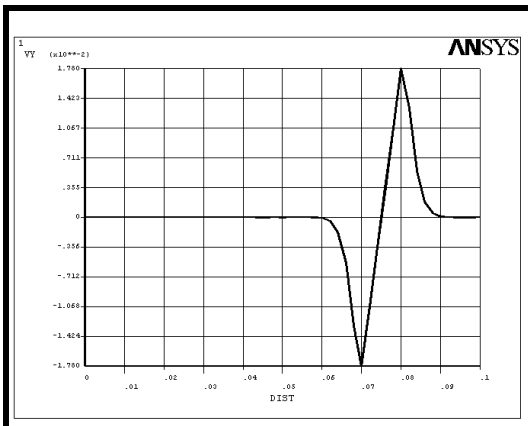

Figure 11. Velocity component in y-direction. Section 1

For the purpose of comparison between transient thermal model with fluid-thermal model, the fluid-thermal model was solved with zero rotational speed.

The result of temperature distribution is show in figure 12.

This figure shows also that the effect of heating load shown in figure 3 has no noticeable affect on the temperature distribution. The temperature distribution is therefore appearing to be symmetric about the workpiece center line. Other data used in fluid-thermal model are presented in table 1 together with transient thermal model.

3.2 Transient Thermal Model with Moving Heat Source.

The fluid-thermal model assumes that the tool is fixed and the plate is moving. The plate movement was modeled by a fluid flow. In transient thermal modeling, the actual tool movement was simulated by assuming a moving heat source. See figure 13. This was accomplished by changing the heat flux location. The tool traveling velocity was assumed constant.

The location of the tool (i.e. heat flux) may be found from the following equation

$$X_{i+1} = X_i + V_t \Delta t \qquad 7$$

Where Δt is the time required for the tool to travel from location X_{i+1} to X_{i+1}. V_t is the tool traveling speed

The temperature distribution is obtained from the law of conservation of energy. Boundary conditions, which were described in section (2.2.1), were implemented. Fluid boundary conditions, which were described in section (2.2.3), were useless. This is because of not including fluid model.

Thermo-physical properties, which were described in section (2.2.2), were used. Heat source starting location was at twice the shoulder radius. Welding process ends at location of three quarter the plate length. Δt was taken as time required for the tool to travel from node (i) to node ($i+1$).

The three dimensional element SOLID70 was selected in the model. SOLID70 has a 3-D thermal conduction capability. The element has eight nodes with a single degree of freedom, temperature, at each node. It is applicable to a 3 dimension, steady–state or transient thermal analysis. In order to include radiation heat transfer, the element SURF152 as used with extra node option. It simulates traditional heat loss to a space node. SURF152 may be used for various load and surface effect applications. It was overlaid onto the upper face of the workpiece. Radiation and convection heat loss was let to be handled by SURF152, while heat flux was applied on SOLID70. Dwell periods was not taken into account in heating process.

Figure 14 shows temperature distribution for the final tool position. Here again there is no significant effect of heat flux variation between advancing and retreating sides (as shown in figure 3) on temperature distribution on those sides.

Temperature distributions for three tool positions are shown in figure 15. It can be seen that the peak temperature is increasing with time. This is because of energy trapping in the workpiece.

Effect of thermal conductivity variation with temperature, as shown in figure 4, on temperature distribution is apparent. It made the distribution wider for higher temperature (i.e. in successive time). This could not be found from fluid-thermal modeling. Other data used are presented in table 1.

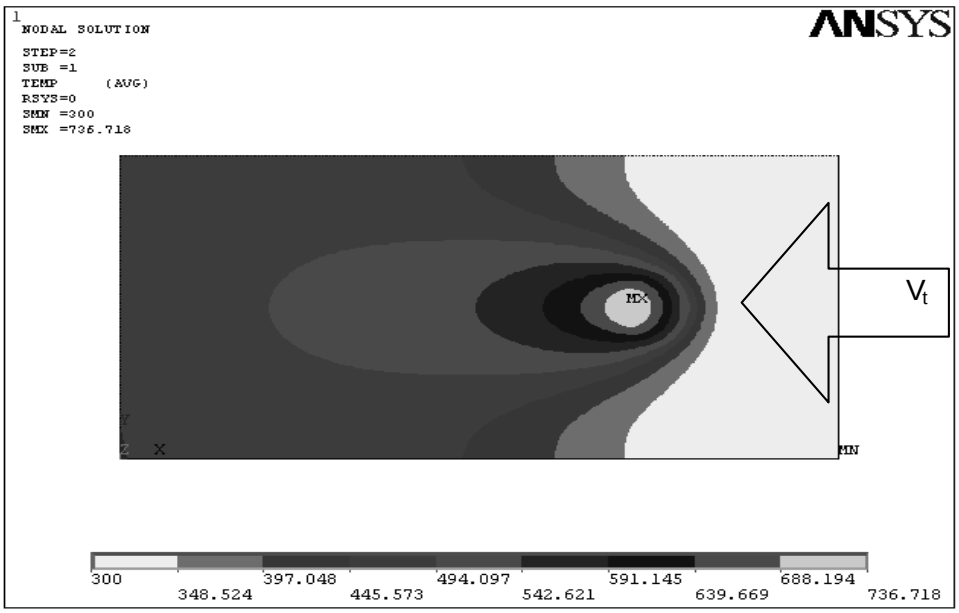

Figure 12. Temperature distribution with no tool rotation

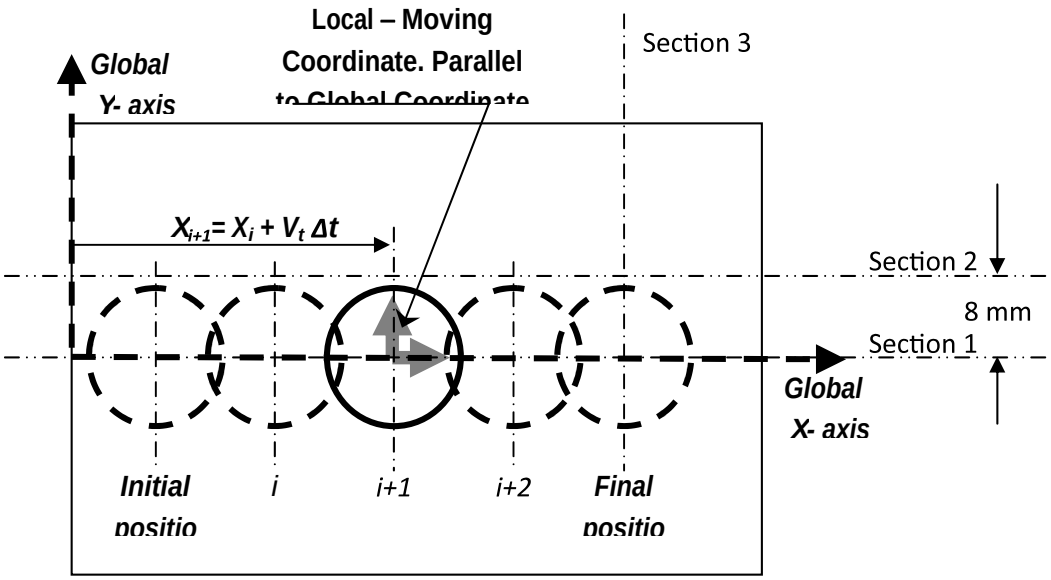

Figure 13. Modeling of heat source movement
at different time steps.

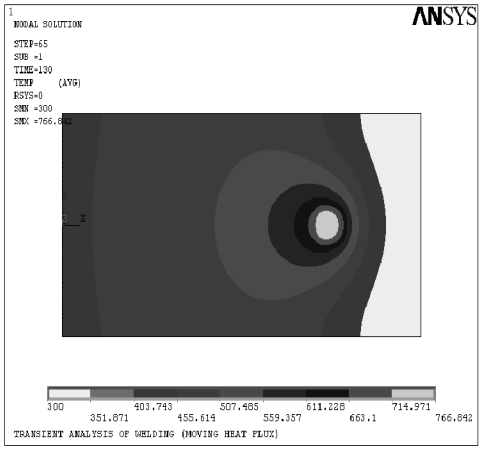

Figure 14. Temperature distribution for moving heat source model

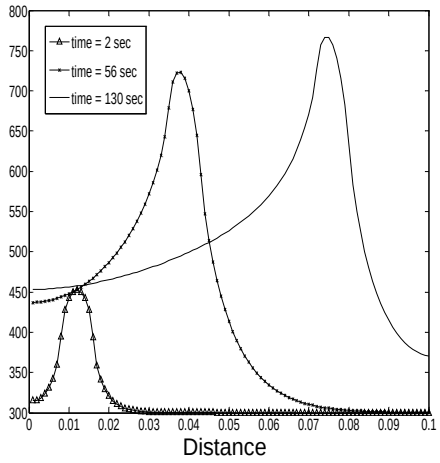

Figure 15. Temperature distributions for three tool positions. Section 2.

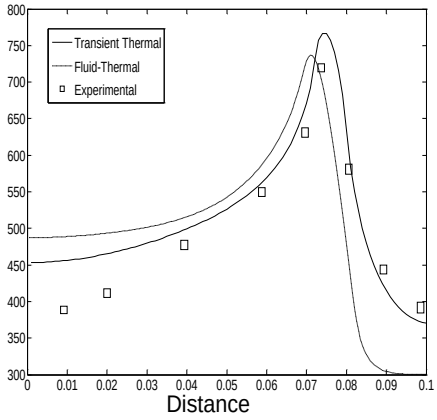

Figure 16. Comparison between experimental [6] and the two models results. Section 2

Table 1. Data used for both models

Plate length = 100 mm
Plate with = 50 mm
Plate thickness = 4 mm
Shoulder radius = 6 mm
h_b = 50 W/m^2.K
h = 30 W/m^2.K
ω = 36 rad/sec
V_t = 1 mm/sec
T_o = 300 K
ε = 0.5
$\sigma = 5.67\times10^{-8}$ W/m^2.K
ρ = 2700 kg/m^3
$\nu = 3\times10^6$ N/m.sec
δ = 0.9

4. Summary and Conclusion

In order to have a full understanding of the FSW process, one has to follow more than one approach. Although for a given approach a predetermined results can be found by adjusting (trail and error) some parameters, but still there should be inherent different characteristics for each model and/or approach that should study.

Friction stir welding process was modeled in this paper by using two approaches. First

approach assumes that the heat flux (tool) is fixed while motion was given to the plate. This was accomplished by the use of fluid-thermal model, in which fluid flow was used to emulate change of heat flux location. Viscosity variation with temperature was neglected in this work since it has no effect on temperature distribution.

In the second approach, the location of the heat flux was changed, while the plate was fixed and modeled as a heat conducting block..

Figure 16 shows a comparison of results obtained hitherto from both models. Also experimental results taken from NANDAN [6] were superimposed on the same graph. Peak temperature resulting from transient thermal analysis is more than experimental results because of the lake of accuracy in modeling of heat transfer. In actual case heat transfer through the fixture will increase the cooling process of the workpiece. Also it is more than that obtained from fluid-thermal model. This because that of energy trapping in transient model while it was released by the fluid leaving downstream the fluid-thermal model.

The results obtained from transient thermal modeling were more accurate than those obtained from fluid-thermal model.

References

[1] W.M. Thomas, E.D. Nicholas, J.C. Needham, M.G. Murch, P. Templesmith, C.J. Dawes, G.B. Patent Application No. 9125978.8 (December 1991).

[2] Pedro Vilac, Lu´ısa Quintino, Jorge F. dos Santos, *i*STIR—Analytical thermal model for friction stir welding, Journal of Materials Processing Technology 169 (2005) 452–465

[3] P. Ulysse, Three-dimensional modeling of the friction stir-welding process,International Journal of Machine Tools & Manufacture 42 (2002) 1549–1557

[4] M. Song, R. Kovacevic, Thermal modeling of friction stir welding in a moving coordinate system and its validation, International Journal of Machine Tools & Manufacture 43 (2003) 605–615

[5] Vijay Soundararajan, Srdja Zekovic, Radovan Kovacevic, Thermo-mechanical model with adaptive boundary conditions for friction stir welding of Al 6061, International Journal of Machine Tools & Manufacture 45 (2005) 1577–1587

[6] R. NANDAN, G.G. ROY, T. DEBROY, Numerical Simulation of Three-Dimensional Heat Transfer and Plastic Flow During Friction Stir Welding,METALLURGICAL AND MATERIALS TRANSACTIONS A,37A, APRIL 2006—1247

[7] CONNOR, J. J. and BREBBIA, C. A., finite element techniques for fluid flow, NEWNES-BUTTERWORTHS,Boston, (1978).

[8] ANSYS v.10 help, ANSYS Theory reference, chapter 14. element library.